

Features in Continuous Parallel Coordinates

Dirk J. Lehmann and Holger Theisel

Abstract—Continuous Parallel Coordinates (CPC) are a contemporary visualization technique in order to combine several scalar fields, given over a common domain. They facilitate a continuous view for parallel coordinates by considering a smooth scalar field instead of a finite number of straight lines. We show that there are feature curves in CPC which appear to be the dominant structures of a CPC. We present methods to extract and classify them and demonstrate their usefulness to enhance the visualization of CPCs. In particular, we show that these feature curves are related to discontinuities in Continuous Scatterplots (CSP). We show this by exploiting a curve-curve duality between parallel and Cartesian coordinates, which is a generalization of the well-known point-line duality. Furthermore, we illustrate the theoretical considerations. Concluding, we discuss relations and aspects of the CPC's/CSP's features concerning the data analysis.

Index Terms—Features, Parallel Coordinates, Topology, Visualization.

1 INTRODUCTION

The visual analysis of data has become important within the last years due to the substantial benefit to facilitate an intuitive data access. Especially approaches based on mappings/projections are popular and widely used, e.g., parallel coordinates, scatterplots or radvis, which all visualize the data discretely.

For some time past, corresponding continuous visualizations are developed which visualize data uninterrupted. Within those visualizations, additional features occur in comparison to the corresponding discrete visualizations. The additional features convey certain properties about the underlying data, are therefore relevant for the visual analysis, and thus need to be understood concerning their causes and meanings. At present, our community knows a few of such continuous visualization approaches but we know not yet much about the features of them.

Two popular examples of continuous visualizations are Continuous Scatterplots [3] and Continuous Parallel Coordinates [14]. Concerning this, article [18] presents a classification of features of Continuous Scatterplots, introduces appropriate detection approaches and gives first rudiments what the meaning of them within the data might be. Furthermore, article [14] shows that Continuous Scatterplots can be straight transformed into Continuous Parallel Coordinates and that they are therefore related to each other.

However, not yet investigated are the features within Continuous Parallel Coordinates which occur, e.g., as edges. Therefore, the theoretical part of our paper completely investigates and describes the mathematical causes of such features, and the practical part of our paper exploits the known features and relations of Continuous Scatterplots and Continuous Parallel Coordinates [14, 18] in order to directly detect and illustrate the discussed features within the Continuous Parallel Coordinates.

In detail, our contributions are:

- a tool/algorithm to generate a linked overlay between the involved visualization domains in order to examine relations between the features (Section 4),
- to describe several categories of features in Continuous Parallel Coordinates (Section 5),
- to reveal relations between features in Continuous Parallel Coordinates and Continuous Scatterplots (Section 5.3.2),

• Department of Simulation and Graphics at the University of Magdeburg, Germany, E-mail: {dirk, theisel}@isg.cs.uni-magdeburg.de

Manuscript received 31 March 2011; accepted 1 August 2011; posted online 23 October 2011; mailed on 14 October 2011.

For information on obtaining reprints of this article, please send email to: tvcg@computer.org.

- applications in order to demonstrate the feature relations of the involved visualization approaches (Section 6), and
- a discussion of the progress concerning the feature-based data analysis with Continuous Scatterplots/Continuous Parallel Coordinates (Section 7).

Following, the related work and background, on which our work is based on, are presented.

2 RELATED WORK & BACKGROUND

In 2008, Bachthaler and Weiskopf [3] presented the visualization approach of Continuous Scatterplots. They extended the concept of discrete scatterplots in order to produce scatterplots which are continuously defined: if the underlying scalar fields are continuous, then the construction of a Continuous Scatterplot (CSP) is possible, as the authors show. Regarding this, a continuous mapping $\tau : \mathbb{R}^n \rightarrow \mathbb{R}^m$ between an n -dimensional space and an m -dimensional space is required to define a scalar density function $\sigma(\tau) : \mathbb{R}^m \rightarrow \mathbb{R}$, which yields color coded the CSP visualization. The first domain \mathbb{R}^n of this map τ is known as *spatial domain* (SD) because the data are measured there. The second domain \mathbb{R}^m is denoted as *data domain* (DD).

To draw an analogy to physics, a mass is defined by an integral over a volume element weighted with a certain density. Thus, considering a small SD volume element $V \in \mathbb{R}^n$ and the corresponding DD volume element $\Phi = \tau(V) \in \mathbb{R}^m$, the CSP approach assigns each of them a mass value by $m_{sd} = \int_V s(\mathbf{x}) \, d^n \mathbf{x}$ (usually $s(\mathbf{x}) = 1$) and $m_{dd} = \int_{\Phi=\tau(V)} \sigma(\boldsymbol{\xi} = \tau(\mathbf{x})) \, d^m \boldsymbol{\xi}$. Under the assumption of mass conservation $m_{sd} = m_{dd}$ the required scalar density function σ can be described implicitly as:

$$\int_V s(\mathbf{x}) \, d^n \mathbf{x} = \int_{\Phi=\tau(V)} \sigma(\boldsymbol{\xi}) \, d^m \boldsymbol{\xi}.$$

Several analytical as well as numerical techniques can be derived from this equation in order to calculate and to render CSPs of most diverse dimensionalities, as shown, e.g., in [2], [4], or [13]. However, the dimensionality of the SD might be an arbitrary value, but the DD is usually two-dimensional as it is typical for a visualization.

Later on, in 2009, Heinrich and Weiskopf [14] presented the visualization approach of Continuous Parallel Coordinates (CPC). They introduced a scheme of continuous density for the concept of parallel coordinates. The approach defines a continuous transformation of the density between the two-dimensional DD and the corresponding two-dimensional *parallel coordinates domain* (PCD) with aid of the point-line duality [15, 17, 16], which describes that a point in the DD corresponds to a line in the PCD and vice versa. Concerning this, a point $\boldsymbol{\eta} = (\eta_1, \eta_2)^T$ of the PCD links to a line \mathbf{L} in the DD, given by:

$$\mathbf{L} : \boldsymbol{\eta}_2 = \mathbf{n} \cdot \boldsymbol{\xi}.$$

Please note that the slope of this line depends on the attribute $\eta_1: \mathbf{n} = (1 - \eta_1, \eta_1)^T$. For the density $\varphi(\eta_1, \eta_2) : \mathbb{R}^2 \rightarrow \mathbb{R}$ of an infinitesimal volume $\eta_2 \in \Omega$ in the PCD results the mass $m_{pcd} = \int_{\Omega} \varphi(\eta_1, \eta_2) d\eta_2$. Furthermore, the mass of the corresponding volume Φ in the DD is $m_{dd} = \int_{\Phi} \sigma(\xi) d^2\xi$. With the assumption of mass conservation $m_{pcd} = m_{dd}$ follows the implicit density description, given by:

$$\int_{\Omega} \varphi(\eta_1, \eta_2) d\eta_2 = \int_{\Phi} \sigma(\xi) d^2\xi. \quad (1)$$

With the aid of the point-line duality Equation (1) can be rewritten to define the density $\varphi(\eta)$ of a point $\eta = (\eta_1, \eta_2)^T$ in the PCD by integration of the density $\sigma(\mathbf{L})$ over the corresponding line \mathbf{L} in the DD:

$$\varphi(\eta_1, \eta_2) = \int_L \frac{\sigma(\mathbf{L}(t))}{\|\mathbf{n}\|} dt. \quad (2)$$

Based on Equation (2) some approaches to render a CPC from a CSP have been introduced. One approach, named *gathering*, determines several density values in the PCD by a Monte Carlo integration of the density over the corresponding lines in DD in order to generate a numerical approximation of the CPC which corresponds to a certain DD. Another approach to get such an approximation is called *scattering*. It takes the backward direction and blends different lines of constant density from samples of the DD onto their corresponding lines in PCD by exploiting the point-line duality. Additionally, a third *analytical approach for triangulated data* is mentioned, which allows an analytical density interpolation from a triangulated grid of the DD, which is mapped onto the corresponding lines of the PCD. In practice, this rendering approach is very usable due to the fact that a CSP is mostly presented as triangulated data.

In 2010, Lehmann and Theisel [18] started the discussion about discontinuity features within CSPs, in order to enhance the user's ability to even better interpret data with the aid of the CSPs. Regarding this, the discontinuities are non-smooth transitions within the scalar field of density, as which a CSP can be interpreted. The authors introduced mathematical models and detection approaches for discontinuities of several cases of CSPs: a CSP^{2D} is based on a map from a two-dimensional SD onto a two-dimensional DD; a CSP^{3D} is based on a map from a three-dimensional SD onto a two-dimensional DD. It has been shown that discontinuities are either caused by effects of the boundary or the mapping function, which connect both involved domains with each other.

For a CSP^{2D} an equivalent parametric surface $S_{\xi,d}$ can be assigned by

$$S_{\xi,d} = \begin{pmatrix} \xi_1 = \tau_1(\mathbf{x}) \\ \xi_2 = \tau_2(\mathbf{x}) \\ d = \det(\mathbf{D}(\tau)(\mathbf{x})) \end{pmatrix}$$

where $\det(\mathbf{D}(\tau)(\mathbf{x}))$ (with the Jacobian \mathbf{D}) codes the reciprocal density value $\sigma(\xi(\mathbf{x}))$ for a DD element $\xi(\mathbf{x}) = \tau(\mathbf{x}) : \mathbb{R}^2 \rightarrow \mathbb{R}^2$. Closed discontinuity curves with infinite density are zero crossings of the surface and the DD described by $S_{\xi,d=0}$. In practice, the SD is bounded. Therefore, further discontinuity curves occur where the boundary edges of the SD are mapped onto the DD. These curves appear as "jumps" within the density. For a CSP^{3D} the discontinuities can be described via a helpful vector field $\mathbf{q}(\mathbf{x}) = \nabla \xi_1(\mathbf{x}) \times \nabla \xi_2(\mathbf{x})$. Curves for which this vector field vanishes $\mathbf{q}(\mathbf{x}) = \mathbf{0}$, mapped onto the DD, are discontinuities. If they fulfill that the eigenvalues λ_1, λ_2 of the Jacobian are $\Re\{\lambda_1\} \leq 0 \leq \Re\{\lambda_2\}$, then they form discontinuity curves with infinite density which are denoted as *saddle discontinuities*. Otherwise they are "jumps" within the density denoted as *center discontinuities*. Furthermore, interesting boundary effects have been mentioned, which also yield density "jumps": the boundary edges of the SD, and the boundary switch curves [28] of the vector field $\mathbf{q}(\mathbf{x})$. We consider that the SD, the DD and the PCD are normalized within a range of $[0, 1]^h$, whereas h is the dimensionality of a certain domain. Figure 1 summarizes the classification of discontinuity features.

In Section 5 ("Features") we discuss similar effects for the Continuous Parallel Coordinates, after giving an overview about the used

		2D	3D	
Infinite Density (Attract Curve)	$S_{\xi,d=0}$	$\mathbf{q}(\mathbf{x}) = 0$ Saddle Discontinuity $\Re\{\lambda_1\} \leq 0 \leq \Re\{\lambda_2\}$		Mapping Effects
Density Jump (Edge Curve)	Boundary Edges	$\mathbf{q}(\mathbf{x}) = 0$ Center Discontinuity $\Re\{\lambda_1\} = \Re\{\lambda_2\} = 0$	Boundary Edges	
			Boundary Switch Curves of $\mathbf{q}(\mathbf{x})$	Boundary Effects

Fig. 1. Classification of discontinuity features for $CSP^{2D/3D}$. Except for the center discontinuities, the boundary generates density jumps and the mapping generates infinite density.

notation and an introduction into the required theory of geometric relations between the DD and the PCD.

3 NOTATIONS & ABBREVIATIONS

Due to the theoretical nature of the paper we use a lot of different mathematical notations and abbreviations which we summarize here.

Domain	Scalar (\mathbb{R})	Vector ($\mathbb{R}^{2/3}$)
Spatial Domain	x, y, z Attributes of Point s Scalar Value/Density	τ^{-1}, \mathbf{x} Point
Data Domain	$\xi_{1/2}$ Attributes of Point μ, ξ Distances σ Scalar Value/Density	τ, ξ Point $\xi(t)$ Curve \mathbf{L} Line/Polyline
Parallel Coordinates Domain	$\eta_{1/2}$ Attributes of Point φ Scalar Value/Density	$\boldsymbol{\eta}$ Point $\boldsymbol{\eta}(t)$ Curve \mathbf{L} Line/Polyline
Not Domain-Specific	λ Eigenvalue t Parameter $c_{1/2}$ Attributes of Center $a_{1/2}$ Constants r Radius of Circle	\mathbf{n} Normal \mathbf{P} Circle \mathbf{c} Center Point \mathbf{v} Tangent (curve) \mathbf{r} Tangent (line)

Fig. 2. Mathematical notations.

Our used mathematical notations are given in Figure 2 and are guided by [3, 14, 13]. Variables related to the spatial domain appear with Latin letters, those which address the data domain or parallel coordinates domain appear with Greek letters. Additionally, lowercase thin variables relate to scalar values and the bold variables relate to vectors with two/three attributes. Uppercase bold variables are lines or curves. Those variables might occur in italic, non-italic or with additional indices for reasons of case differentiation.

As mentioned in the related work, we consider three different domains (see Figure 3). Regarding this, a CSP is defined by its density σ over the data domain (DD), and a CPC by its density φ over the parallel coordinates domain (PCD). A CSP based on a 2D/3D spatial domain is a $CSP^{2D/3D}$. Certain feature curves within a CSP/CPC appear either as discontinuity curves of density "jumps", which we denote as *edges curves*, or they appear as discontinuity curves of an infinite density which we denote as *attract curves*. Furthermore, feature curves might appear as extreme curves, e.g., ridge curves.

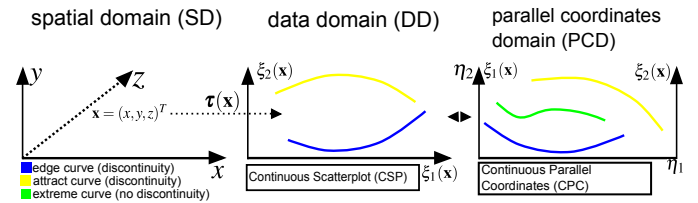


Fig. 3. Considered domains and relations to continuous visualizations.

4 THEORY

In order to understand the relations between the features of the different domains, several geometric properties are introduced at first. By now, the point-line duality is already known (Section 2). In this section we introduce the *curve-curve duality* and the *circle-area duality* which are based on the ellipse-hyperbola duality known, e.g., from [15].

4.1 Curve-Curve Duality

The curve-curve duality [15, 24] means that a curve of the PCD maps exactly onto a curve in the DD and vice versa.

Proof: let us consider a plain curve $\xi(t) : \mathbb{R} \rightarrow \mathbb{R}^2; t \in \mathbb{R}$ in the DD with the tangent vector $d\xi(t)/dt = \dot{\xi}(t)$, which define a tangent line $L(t)$. Due to the point-line duality the line $L(t)$ maps to a point curve $\eta(t)$ in the PCD. Consequently, curve $\xi(t)$ and curve $\eta(t)$ link to each other. The same idea applies for the proof of the backward direction from PCD to DD.

4.1.1 Curve in PCD from Curve in DD

At first, we reveal a curve $\eta(t) = (\eta_1(t), \eta_2(t))^T$ from curve $\xi(t) = (\xi_1(t), \xi_2(t))^T$. The tangent line $L(t)$ is given by: $L(t) = \xi(t) + t_{dd} \dot{\xi}(t); t_{dd} \in \mathbb{R}$. The line points $\xi(t)$ and $\xi_\Delta(t) = \xi(t) + \dot{\xi}(t)$ yield two lines in the PCD, given by:

$$\begin{aligned} L_{\xi(t)} &= \left(\begin{array}{c} a_1 \\ \xi_1(t) \end{array} \right) + t_1 \left(\begin{array}{c} a_2 - a_1 \\ \xi_2(t) - \xi_1(t) \end{array} \right); t_1 \in \mathbb{R}, \\ L_{\xi_\Delta(t)} &= \left(\begin{array}{c} a_1 \\ \xi_{\Delta_1}(t) \end{array} \right) + t_2 \left(\begin{array}{c} a_2 - a_1 \\ \xi_{\Delta_2}(t) - \xi_{\Delta_1}(t) \end{array} \right); t_2 \in \mathbb{R}. \end{aligned}$$

As Figure 4 clarifies, the intersection point $L_{\xi(t)} = L_{\xi_\Delta(t)}$ of both lines

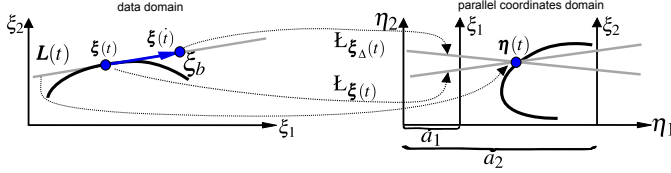


Fig. 4. Construction diagram of a curve in PCD from a curve in DD.

is the corresponding point $\eta(t)$ in the PCD, given by:

$$\left(\begin{array}{c} a_1 \\ \xi_1(t) \end{array} \right) + t_1 \left(\begin{array}{c} a_2 - a_1 \\ \xi_2(t) - \xi_1(t) \end{array} \right) = \left(\begin{array}{c} a_1 \\ \xi_{\Delta_1}(t) \end{array} \right) + t_2 \left(\begin{array}{c} a_2 - a_1 \\ \xi_{\Delta_2}(t) - \xi_{\Delta_1}(t) \end{array} \right). \quad (3)$$

Solving Equation (3) and inserting the result into the equation for line $L_{\xi(t)}$ yields curve $\eta(t)$ in the PCD:

$$\eta(t) = \left(\begin{array}{c} \eta_1(t) \\ \eta_2(t) \end{array} \right) = \left(\begin{array}{c} a_1 \\ \xi_1(t) \end{array} \right) + \left[\frac{\xi_1(t)}{\xi_1(t) - \xi_2(t)} \right] \left(\begin{array}{c} a_2 - a_1 \\ \xi_2(t) - \xi_1(t) \end{array} \right). \quad (4)$$

4.1.2 Curve in DD from Curve in PCD

In order to reveal curve $\xi(t) = (\xi_1(t), \xi_2(t))^T$ from curve $\eta(t) = (\eta_1(t), \eta_2(t))^T$ we consider the inverse direction. Figure 5 shows that

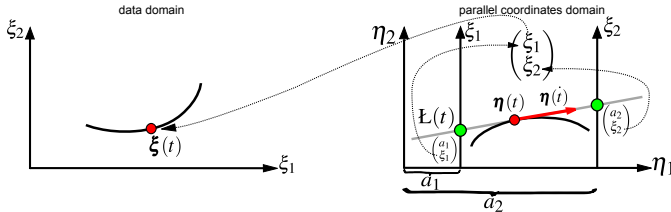


Fig. 5. Construction diagram of a curve in DD from a curve in PCD

the horizontal ξ -axes in PCD coordinates are given by: $(a_i, t)^T; t \in$

$\mathbb{R}, i = \{1, 2\}$. The tangent line $L(t)$ of the curve $\eta(t)$ is given by: $L(t) = \eta(t) + t_{pcd} \dot{\eta}(t); t_{pcd} \in \mathbb{R}$. The components of the curve $\xi(t)$ in DD are now defined through the second attribute of the intersection points between the tangent line $L(t)$ and the ξ -axes in the PCD, given by the linear system $L(t) = (a_i, t)^T$:

$$\eta(t) + t_{pcd} \dot{\eta}(t) = \left(\begin{array}{c} a_i \\ t \end{array} \right). \quad (5)$$

Solving Equation (5) yields $t_{pcd} = \frac{a_i - \eta_1(t)}{\dot{\eta}_1(t)}$, which – inserted in the equation for tangent line L – gives the formula for curve $\xi(t)$:

$$\xi(t) = \left(\begin{array}{c} \xi_1(t) \\ \xi_2(t) \end{array} \right) = \left(\begin{array}{c} \eta_2(t) + \frac{a_1 - \eta_1(t)}{\dot{\eta}_1(t)} \eta_2(t) \\ \eta_2(t) + \frac{a_2 - \eta_1(t)}{\dot{\eta}_1(t)} \eta_2(t) \end{array} \right). \quad (6)$$

For the paper, we consider only the PCD standard configuration [15] with $a_1 = 0$ and $a_2 = 1$.

4.2 Circle-Area Duality

By the curve-curve duality the point-line duality is extensible to a concept of circle-area duality, as shown in Figure 6. It describes that an area of a circle in one domain is linked to an area bounded by the corresponding curve of the other domain. The proof is trivial, thus

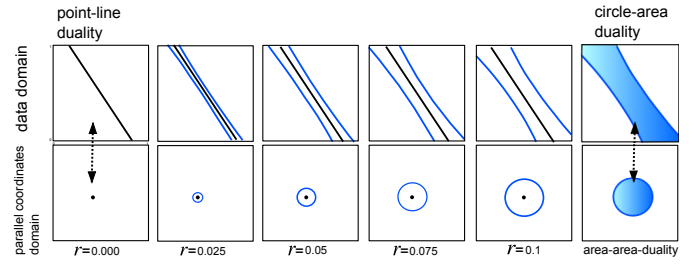


Fig. 6. The circle-area duality illustrated for the case of PCD onto DD.

we mention only the basic scheme of it: two circles with different radii but same center point in one domain are related to two curves in the other domain which are free of intersections (curve-curve duality). Additionally, a circle with radius $r = 0$ links to a corresponding line of the center point (point-line duality). By converging an arbitrary radius $r \rightarrow 0$ the circle-area duality follows directly.

We briefly treat the case from the PCD to the DD. Let $\mathbf{P}_c^r(t) = (r \cdot \cos(t) + c_1, r \cdot \sin(t) + c_2)^T; t \in \{0, 2\pi\}$ be a circle within the PCD with the center $\mathbf{c} = (c_1, c_2)^T$ and the radius r . Then, concerning Equation (6), the curve $\xi_c^r(t)$ in the DD, which envelopes the corresponding area, is given by:

$$\xi_c^r(t) = \left(\begin{array}{c} \frac{c_2 \cdot \sin(t) + c_1 \cdot \cos(t) + r}{\sin(t)} \\ \frac{c_2 \cdot \sin(t) - c_1 \cdot \cos(t) + r}{\sin(t)} \end{array} \right). \quad (7)$$

Now we treat the case from the DD onto the PCD. We consider a circle $\xi_c^r(t) = (r \cdot \cos(t) + c_1, r \cdot \sin(t) + c_2)^T$ in the DD. With Equation (4) its corresponding curve in the PCD is:

$$\mathbf{P}_c^r(t) = \left(\begin{array}{c} \frac{\sin(t)}{\sin(t) + \cos(t)} \\ \frac{c_1 \cdot \cos(t) + c_2 \cdot \sin(t) + r}{\sin(t) + \cos(t)} \end{array} \right).$$

4.2.1 Circle-Area linked overlay Algorithm

What remains is to state an algorithm to link/highlight associated areas. We introduce it for the case from the PCD to the DD, the other case works analogous. The user interactively places a circle \mathbf{P}_c^r with center \mathbf{c} and radius r in the PCD. The linked area can be obtained as

follows: the corresponding curve $\xi_c^r(t)$ (c.f. Equation (7)) is approximately drawn as polyline \mathbf{L} , where one line segment \mathbf{L}_i is given by the points $(\xi_c^r(t_i), \xi_c^r(t_{i+1}))$ with $t_{i+1} = t_i + h$ (h steers the resolution). The clipping between polyline \mathbf{L} and the domain boundary edges, given by the CohenSutherland or the LiangBarsky technique, yields a polygon which represents the area in DD. We know that the line \mathbf{L}_c of the center point c is inside of this area. Thus, the polygon can be filled by rasterizations [10], as the edge-fill-algorithm [1] or brute-force with a flood-fill seeded at \mathbf{L}_c . This linking of the areas is shown exemplarily in the applications (Section 6).

5 FEATURES

A CPC equates to a two-dimensional scalar field, caused by the transformation of the DD onto the PCD. Thus, known scalar field features might occur, cf. [7, 9, 21]. Additionally, the investigation of the feature's relations is important to facilitate the visual analysis of data by CPCs. In this section we investigate the boundary features, the local features as well as the global features.

5.1 Boundary Features

Figure 7 illustrates the relations of the boundary: the boundary edges of the DD map to the corner points of the PCD. The boundary corner points left-down/right-up of the DD map to the upper/downer boundary edges of the PCD. Thus, these domain structures are not able to mutually influence the quality of the corresponding visualization because they are just barely visible by the user. In contrast, the right-down/left-up corner points map to diagonal lines which lie across the visualization. The intersection point of these diagonal lines generates a corresponding diagonal line within the DD.

Consequently, the transformation from DD to PCD causes that certain areas of one domain visually affect certain areas of the other domain stronger than other areas. Concerning this, the distribution of gray-scale values of Figure 7 visually links the areas of DD and PCD which mutual affects strongest; marked by similar gray-scale values.

Thus, for instance noise within the DD near the right-down/left-up corner points would be mapped more in the center of the PCD, in contrast to noise close to the other corner points. In other words: the closer the density values of a CSP to the right-down/left-up corner points are, the more they influence the visual quality of the CPC. Furthermore, a CPC is not invariant of rotations of the corresponding CSP. Similar effects are already known from the discrete parallel coordinates.

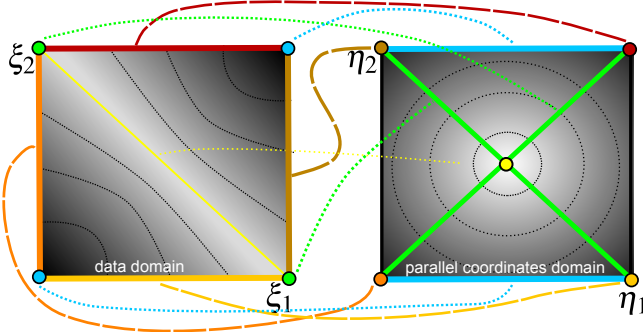


Fig. 7. Relations between domain boundary features, as boundary edges and corner points: the relations are indicated by corresponding colors. Regions with same gray value affect each other stronger than other regions.

5.2 Local Features

In this section we investigate the relations between the DD's local features and the CPC. The DD's local features [5] of an arbitrary 2D scalar field $\sigma(\xi)$ are given by $\nabla\sigma(\xi) = \mathbf{0}$, where $0 < \lambda_1 \leq \lambda_2$ gives a minimum (source), $\lambda_1 < 0 < \lambda_2$ gives a saddle, and $\lambda_1 \leq \lambda_2 < 0$ gives a maximum (sink), whereas $\lambda_{1,2} = \frac{\sigma_{\xi_1\xi_1} + \sigma_{\xi_2\xi_2}}{2} \pm \sqrt{\frac{1}{4}(\sigma_{\xi_1\xi_1} - \sigma_{\xi_2\xi_2})^2 + \sigma_{\xi_2\xi_1}^2}$ are the eigenvalues of the

Hessian of σ with the partial derivatives σ_{ij} ; $i, j \in \{\xi_1, \xi_2\}$. Such local features are especially important for the numerous visualization and analysis approaches which are based on the Morse-Smale Complex [11, 12]. Several local feature detection approaches such as [9, 7] are already known. Thus, we do not treat this aspect.

Two cases are possible: features with a finite scalar value and features with an infinite scalar value. The last case are isolated singularities of the scalar field. Based on the point-line duality the question arises whether those local features form characteristic lines in CPC.

The case of local features with a finite scalar value does not, as we will briefly explain: the feature's curvature, given by κ , describes the behavior of the environed scalar values. If κ is small, the feature's scalar value is similar to the scalar values of its ε -environment and causes lines with similar density in the CPC, which strongly visually influence each other. The more κ grows, the more distinct is the corresponding line of a feature within the CPC, in comparison to lines of the ε -environment. But this is not a stable property in order to characterize local feature lines in general. Thus, this kind of local features might produce visible lines, but this is neither a stable property nor a characteristic structure.

Unlike, the case of local singularity features of a scalar field. They would cause characteristic CPC lines with an infinite density. Thus, we further need to consider the special case of such singularities caused by $\text{CSP}^{2D/3D}$. The attract curves of a CSP^{2D} are curves of the parametric surface with $S_{\xi,d=0}$ (cf. Section 2). The attract curves of a CSP^{3D} are the feature lines of the vector field \mathbf{q} . Both structures depend on the scalar functions $\xi_1 = \tau_1(\mathbf{x})$ and $\xi_2 = \tau_2(\mathbf{x})$. By varying one of these functions, both structures might shrink to a single point during their evolution (Figure 8). Then, the CSP's attracted curves form local isolated singularities. By a small variation or by adding noise these singularities would break and are not stable within the attracted curve life cycle. Thus, isolated singularities in σ are not relevant concerning $\text{CSP}^{2D/3D}$.

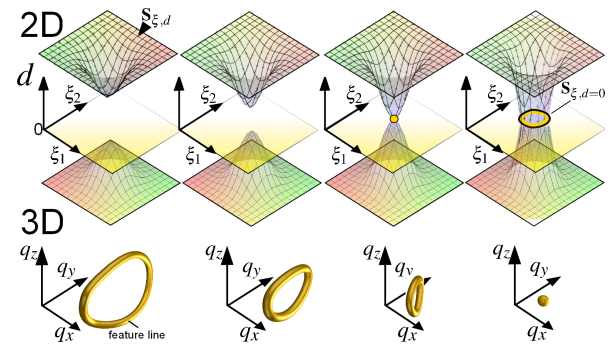


Fig. 8. Evolution to isolated singularities for $\text{CSP}^{2D/3D}$: (up) a curve $S_{\xi,d=0}$ of the 2D case or (down) a feature line of the 3D case might shrink to a single point, which would cause an isolated singularity within the CSP. This is unstable and would break by adding noise.

5.3 Global Features

In this section, we investigate the relations of global features between the DD and the CPC. Such global features are mainly discontinuity curves which either form edge curves or attract curves. At first, we treat the case of a generic scalar field $\sigma(\xi)$, given over the DD. Afterwards, we explore the behavior between the $\text{CSP}^{2D/3D}$ and the CPC as special cases of scalar fields.

5.3.1 Global Features in CPC based on generic Scalar Fields

Given: a DD discontinuity curve by $\xi(t) = (\xi_1(t), \xi_2(t))^T$. Within an infinitesimal region, the curve's behavior can be described by the

(semi) osculating circle $\mathbf{P}_c^r(t)$ with radius $r(t)$ and center $\mathbf{c}(t)$:

$$r(t) = \frac{(\xi_1(t)^2 + \xi_2(t)^2)^{\frac{3}{2}}}{\det(\xi(t), \ddot{\xi}(t))}, \mathbf{c}(t) = \begin{pmatrix} \xi_1(t) - \frac{\xi_2(t) \cdot (\xi_1(t)^2 + \xi_2(t)^2)}{\det(\xi(t), \ddot{\xi}(t))} \\ \xi_2(t) - \frac{\xi_1(t) \cdot (\xi_1(t)^2 + \xi_2(t)^2)}{\det(\xi(t), \ddot{\xi}(t))} \end{pmatrix}.$$

In order to simplify the considerations below, we place the ordinate's origin in $\mathbf{c}(t)$ and we consider the circle's system as aligned with the ξ axes.

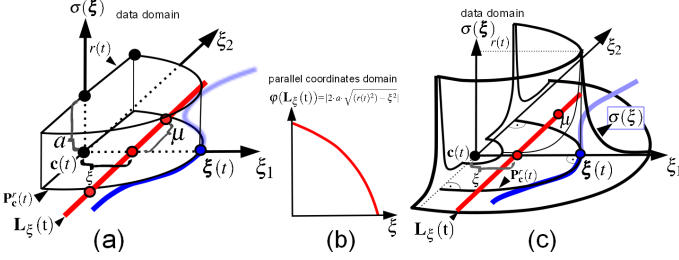


Fig. 9. Discontinuity Curves: (a) mathematical relations for edge curves in DD, (b) behavior of the density φ of a CPC at a DD edge curve. An edge curve in DD is not an edge curve in CPC. (c) The mathematical relations for curves with infinite scalar value in DD.

Let us assume that the discontinuity curve $\xi(t)$ is an edge curve. Then, the edge curve can be locally described as a disk of a high $\sigma(\xi) = a \in \mathbb{R}$ over the osculating circle $\mathbf{P}_c^r(t)$ ($\sigma(\xi) = 0$ else). Figure 9 (a) illustrates this. The density $\varphi(\mathbf{L}_\xi(t))$ in PCD of a (vertical) line $\mathbf{L}_\xi(t)$ in DD, where ξ is the (horizontal) distance to $\mathbf{c}(t)$ and $\mu = \sqrt{r(t)^2 - \xi_1^2}$, is given by (cf. Equation (2)):

$$\varphi(\mathbf{L}_\xi(t)) = |2 \cdot a \cdot d\mu| = |2 \cdot a \cdot \sqrt{(r(t)^2) - \xi^2}|.$$

This is a monotonically decreasing density function (Figure 9 (b)) for $\xi \in \{0, \infty\}$. Therefore, an edge curve in DD is not mapped onto an edge curve in PCD, i.e., the edge disappears. We denote this as *smoothness effect*, which informally means: an edge in DD is smoothed by the CPC's transformation.

Let us now assume that the discontinuity curve $\xi(t)$ is an attract curve. Then, the behavior of this curve can be locally described by its osculating circle $\mathbf{P}_c^r(t)$. The scalar value $\sigma(\xi)$ at distance ξ along the ξ_1 axis can be described as $\sigma(\xi) = 1/|r(t) - \xi|^a$, so that the scalar value is infinite at the periphery of the osculating circle. We assume this kind of functional behavior for each center line of $\mathbf{P}_c^r(t)$, which is orthogonal to the periphery (Figure 9 (c)). For each distance μ on a (vertical) line $\mathbf{L}_\xi(t)$, the scalar value $\sigma_\mu(\xi)$ is given by the shortest distance between the corresponding line point $\mathbf{L}_{\xi,\mu}(t)$ and the periphery: $\sigma_\mu(\xi) = |(|\mathbf{L}_{\xi,\mu}(t)| - r(t))|^{-a}$. Thus, the density $\varphi(\mathbf{L}_\xi(t))$ in PCD for a line $\mathbf{L}_\xi(t)$ in DD is given by:

$$\varphi(\mathbf{L}_\xi(t)) = \int_{\mu} |\sqrt{(\mu^2 + \xi^2)} - r(t)|^{-a} d\mu. \quad (8)$$

This integral cannot be solved analytically. Nevertheless, the density behavior strongly depends on the exponent a . If $a \geq 1$ for $\xi \in \{0, r(t)\}$, the density φ is infinite for each line $\mathbf{L}_\xi(t)$: the attract curve in DD maps onto a region in PCD with infinite density. If $a \geq 1$ for $\xi = r(t)$ and $0 \leq a < 1$ else, then, each tangent line gives an infinite density, the other lines do not. Due to the curve-curve duality, such a curve maps onto a curve in PCD with infinite density. If $a \geq 1$ for $\xi \in \mathbb{R}$, then, there is no line with infinite density in PCD. Thus, such a curve maps on a smooth density plateau in the PCD. Subsequently, we investigate solutions of Equation (8) for the $\text{CSP}^{2D/3D}$ as special case of a scalar field in DD.

5.3.2 Global Features in CPC based on $\text{CSP}^{2D/3D}$

We need to distinguish between feature curves which are caused by a two-dimensional SD, i.e., the DD's scalar field is a CSP^{2D} ; and feature curves which are caused by a three-dimensional SD, i.e., the DD's scalar field is a CSP^{3D} . We assume the knowledge about vector field topology as [26, 20, 27, 25]. Furthermore, note that the CSP's features based on boundary effects (cf. Figure 1) form invariable edge curves and disappear generally within the CPC due to the smoothness effect.

Contour Integral We introduce the concept of *contour integral* for a 2D or 3D scalar field. We will use it to characterize feature curves in CPC.

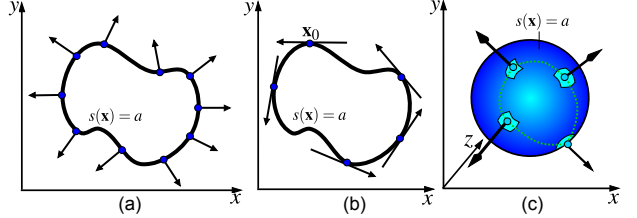


Fig. 10. Contour Integral of the case 2D (a,b) and 3D (c).

definition 1 Given is a scalar field $s(\mathbf{x})$ in SD and a threshold a . The contour integral f of s and a is defined as the integration of $\frac{1}{\|\nabla s\|}$ over the isocontour $s(\mathbf{x}) = a$:

$$f(s, a) = \int_{s(\mathbf{x})=a} \frac{1}{\|\nabla s\|} d\mathbf{x}. \quad (9)$$

For a 2D field s , f is obtained by integrating $\frac{1}{\|\nabla s\|}$ over one (or more) isolines in arc length parametrization. Figure 10 (a) illustrates this. There is an alternative way to compute f : integrate the co-gradient field of s from a point \mathbf{x}_0 on the contour $s(\mathbf{x}) = a$, $f(s, a)$ is the time until it returns to \mathbf{x}_0 again (or it leaves the domain in both forward and backward direction). Figure 10 (b) illustrates this.

For a 3D scalar field s , f is obtained by integrating $\frac{1}{\|\nabla s\|}$ over an isosurface in a local area-preserving parametrization. Figure 10 (c) illustrates this.

The contour in integral gives a well-defined value as long as ∇s does not vanish. However, in order to analyze feature curves in CPC, we are especially interested in the behavior of f at critical points of s . We analyze this by considering a second order approximation of s having a critical point at $\mathbf{0}$ and a Hessian whose eigenvectors λ_i are aligned with the coordinate axes:

$$s(\mathbf{x}) = \frac{\lambda_1}{2} x^2 + \frac{\lambda_2}{2} y^2 + \frac{\lambda_3}{2} z^2$$

where $f(s, 0)$ is the particular point of interest. Fortunately, for this Equation (9) has a closed form solution¹ which gives the following cases: 2D: if $s(0)$ is a local maximum (i.e., $\lambda_1, \lambda_2 > 0$), $f(s, a)$ has a discontinuity at 0. Figure 11 (a) illustrates this. A similar statement holds for a local minimum. If $s(0)$ forms a local saddle, (i.e., $\lambda_1, \lambda_2 < 0$), then $f(s, a)$ diverges to infinity for $a \rightarrow 0$. Figure 11 (b) illustrates this.

3D: if $s(0)$ is a local maximum (i.e., $\lambda_1, \lambda_2, \lambda_3 > 0$), then $f(s, 0) = 0$ and linearly growing with a . Figure 11 (c) illustrates this. A similar statement holds for a local minimum. If $s(0)$ forms a local saddle, (i.e., $\lambda_1, \lambda_2, \lambda_3 < 0$), then $f(s, a)$ has a local finite maximum at $a = 0$. Figure 11 (d) illustrates this.

Note that the asymptotic behavior of f around critical points in s is different in 2D and 3D. Now we establish the relation of feature lines in CSP and CPC by:

¹We computed it by a formula manipulation system like Maple.

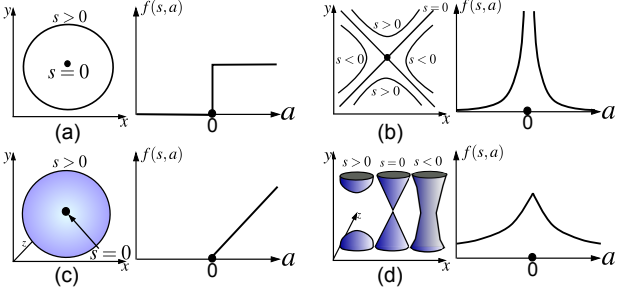


Fig. 11. Behavior of the contour integral at critical points: 2D center/saddle case (a-b) and 3D center/saddle case (c-d).

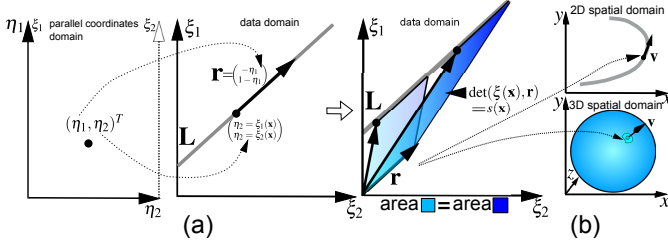


Fig. 12. Relation of the domains. (a) A PCD's point yields a line in DD. (b) The spanned area in DD yields a scalar field in SD.

lemma 1 The density $\varphi(\boldsymbol{\eta})$ at a point $\boldsymbol{\eta} = (\eta_1, \eta_2)^T$ in the PCD is $f(s, a)$ with

$$s(\mathbf{x}) = \det \begin{pmatrix} \xi_1(\mathbf{x}) & -\eta_1 \\ \xi_2(\mathbf{x}) & 1 - \eta_1 \end{pmatrix}, a = \eta_2.$$

Proof: Due to the point-line duality, the point (η_1, η_2) in the PCD corresponds to the line $\det \begin{pmatrix} \xi_1(\mathbf{x}) & -\eta_1 \\ \xi_2(\mathbf{x}) & 1 - \eta_1 \end{pmatrix} = \eta_2$ in implicit form in the DD (Figure 12 (a)). Its integration in SD gives the lemma (Figure 12 (b)). Furthermore, this lemma directly gives us the correlation between feature lines in CSP and CPC both in 2D and 3D.

Case of CSP^{2D} Based on the counter integral, we discuss the CSP^{2D} case in more detail now. A tangent vector $\mathbf{r} = (-\eta_1, 1 - \eta_1)^T$ of a line \mathbf{L} in DD yields, with the Jacobian $\mathbf{D} = \mathbf{D}(\tau(\mathbf{x}))$, a tangent vector \mathbf{v} of the corresponding curve in SD:

$$\mathbf{v} = \begin{pmatrix} \tau_{1_x} & \tau_{1_y} \\ \tau_{2_x} & \tau_{2_y} \end{pmatrix}^{-1} \cdot \mathbf{r} = \begin{pmatrix} \tau_{2_y} & -\tau_{1_y} \\ -\tau_{2_x} & \tau_{1_x} \end{pmatrix} \cdot \det(\mathbf{D}).$$

The co-gradient $\nabla^{-1}\mathbf{s}(\mathbf{x})$ for a certain threshold η_2 , concerning the contour integral, is then defined through:

$$\nabla^{-1}\mathbf{s}(\mathbf{x}) = \nabla^{-1} \det \begin{pmatrix} \xi_1(\mathbf{x}) & -\eta_1 \\ \xi_2(\mathbf{x}) & 1 - \eta_1 \end{pmatrix} = \mathbf{v} \cdot \det(\mathbf{D}).$$

The density in DD [3] is given by: $\sigma = \det(\mathbf{D})^{-1}$. Two properties directly follow: (i) the vector length $\|\nabla^{-1}\mathbf{s}(\mathbf{x})\|$ corresponds to the DD's density, and (ii) an integration curve of $\nabla^{-1}\mathbf{s}(\mathbf{x})$ equates to a certain curve in the SD, whose integration time t_φ gives the PCD's density $\varphi(\mathbf{L}) = \varphi(\boldsymbol{\eta})$ for a certain line \mathbf{L} of the DD (cf. Equation (2)). This way, all domains are related to each other.

As suggested in the contour integral's discussion, we have to treat the critical points. Due to (i), critical points in $\nabla^{-1}\mathbf{s}(\mathbf{x}) = \mathbf{0}$ are also discontinuity points in DD: $\sigma(\boldsymbol{\xi}) = \infty$. There, two behaviors are possible (Figure 14 (a)): a center or a saddle behavior. For a center behavior, the integration time t_φ , and thus the density $\varphi(\boldsymbol{\eta})$ in PCD, in the center's environment is constant (in a first order approximation), and gets abruptly to 0 at the critical point. Hence, for the center case, the DD's

discontinuity point $\boldsymbol{\xi}$ with $\sigma(\boldsymbol{\xi}) = \infty$ corresponds to a point $\boldsymbol{\eta}$ in PCD which is a “jump” within the density φ . For a saddle behavior, the integration time t_φ is infinite at the saddle's streamline: $t_\varphi = \infty$. Hence, for the saddle case, the DD's discontinuity point $\boldsymbol{\xi}$ with $\sigma(\boldsymbol{\xi}) = \infty$ corresponds to a point $\boldsymbol{\eta}$ in PCD with an infinite density: $\varphi(\boldsymbol{\eta}) = \infty$.

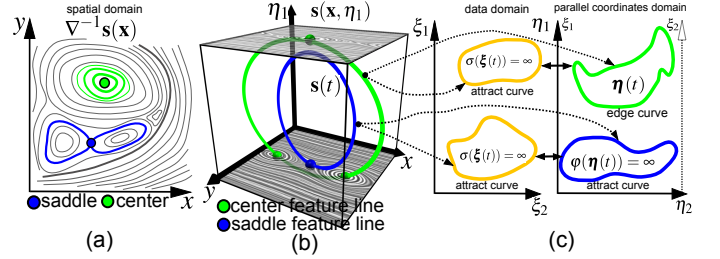


Fig. 14. Relations of global features between CSP^{2D} and a CPC. (a) Co-gradient field of $s(\mathbf{x})$, (b) a feature line in $s(\mathbf{x}, \eta_1)$ yields (c) a DD's attract curve, and at a center/saddle a PCD's edge/attract curve.

Let us now consider a 3D vector field $\mathbf{s}(\mathbf{x}, \eta_1)$ concerning the whole range of tangent vectors $\mathbf{r} = (-\eta_1, 1 - \eta_1)^T$. This vector field is a stack, where each slice η_1 is a single 2D vector field $\nabla^{-1}\mathbf{s}(\mathbf{x})$ of $\mathbf{r} = (-\eta_1, 1 - \eta_1)^T$. In this way, SD, DD, and PCD are combined with each other. The critical points form closed curves in $\mathbf{s}(\mathbf{x}, \eta_1)$, so-called *feature lines* [27], which Figure 14 (b) illustrates. Let $\mathbf{s}(t) = (x(t), y(t), \eta_1(t))^T$ be a feature line of $\mathbf{s}(\mathbf{x}, \eta_1)$: due to (i) it links to a DD attract curve

$$\boldsymbol{\xi}(t) = (\xi_1 = \tau_1(x(t), y(t)), \xi_2 = \tau_2(x(t), y(t)))^T.$$

In addition, the feature line $\mathbf{s}(t)$ links to a curve in the PCD

$$\boldsymbol{\eta}(t) = (\eta_1(t), s(x(t), y(t), \eta_1(t)))^T.$$

If feature line $\mathbf{s}(t)$ has a center behavior, then $\boldsymbol{\eta}(t)$ is an edge curve. If $\mathbf{s}(t)$ has a saddle behavior, then $\boldsymbol{\eta}(t)$ is an attract curve: $\varphi(\boldsymbol{\eta}(t)) = \infty$. Finally, due to transitivity, a CSP^{2D} discontinuity curve $\boldsymbol{\xi}(t)$ links to a discontinuity curve $\boldsymbol{\eta}(t)$ in the corresponding CPC, which is summarized in Figure 14 (c).

Case of CSP^{3D} Based on the counter integral, we discuss the CSP^{3D} case in more detail now. Unlike the previous case, the SD is three-dimensional. Thus, a DD line \mathbf{L} maps onto a surface within vector field $\mathbf{q} = \nabla\xi_1 \times \nabla\xi_2$ [18], given over the SD. The discontinuities of a CSP^{3D} correspond to feature lines in \mathbf{q} . Hence, the density $\varphi(\boldsymbol{\eta}) = \varphi(\mathbf{L})$ in the PCD is given by the integration over the corresponding surface area in \mathbf{q} . All domains are now related to each other.

It is not a trivial task to calculate this area, but the behavior of the surface area strongly depends on the area's evolution in the environment of the critical point in \mathbf{q} . Therefore, using the contour integral for a 3D scalar field s gives this evolution behavior.

The 3D scalar field s of the contour integral $f(s, \eta_1)$, concerning a certain DD's tangent vector $\mathbf{r} = (-\eta_1, 1 - \eta_1)^T$, is given by

$$s(\mathbf{x}) = \det \begin{pmatrix} \xi_1(x, y, z) & r_x \\ \xi_2(x, y, z) & r_y \end{pmatrix}.$$

Each line \mathbf{L} in the DD with constant \mathbf{r} belongs to an iso-surface in $s(\mathbf{x})$. The vector field $\nabla s(\mathbf{x})$ codes the area's contributions for the line \mathbf{L} . In contrast to \mathbf{q} , the critical points in $\nabla s(\mathbf{x})$ are isolated points, with the property that a critical point in $\nabla s(\mathbf{x})$ lies on a feature line in \mathbf{q} , but not vice versa: $\nabla s(\mathbf{x}) = \mathbf{0} \rightarrow \mathbf{q} = \mathbf{0}$. Note: Would one collect and join the critical points of $\nabla s(\mathbf{x})$ for the whole range of \mathbf{r} , one would reveal the feature lines of \mathbf{q} . This way, vector field $\mathbf{s}(\mathbf{x})$ and \mathbf{q} are related to each other, i.e., the one is a kind of decomposition of the other. However, a line \mathbf{L} which touches a DD's discontinuity point corresponds to a critical point in $\nabla s(\mathbf{x})$. Thus, we need to investigate the behavior of the integral contour at the critical points.

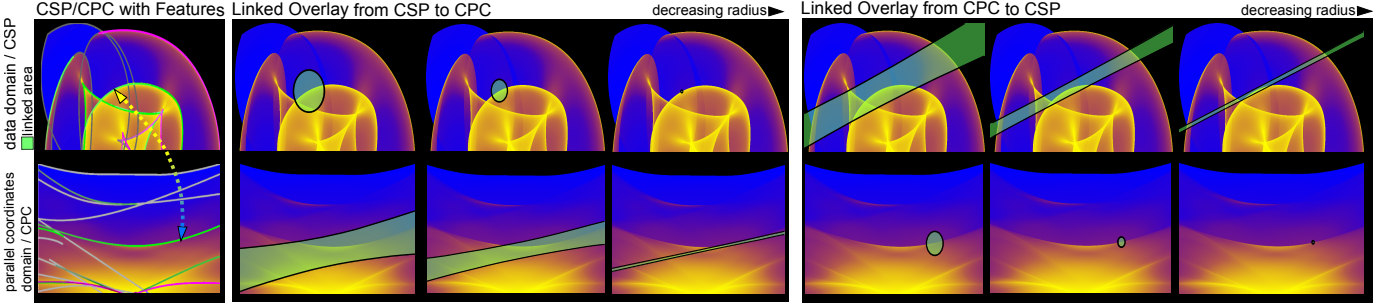


Fig. 13. Linked Overlay Tool: feature points in one domain link mutual onto tangent lines of corresponding feature points in the other domain.

Two kinds of critical points in $\nabla s(\mathbf{x})$ are possible: a center or a saddle critical point. Please note that a center in $\nabla s(\mathbf{x})$ appears if the corresponding point on a feature line in \mathbf{q} is also a center discontinuity. The same applies for a saddle.

A center critical point corresponds to the introduced 3D maximum behavior of the contour integral $f(s, \eta_1)$: the density φ is linearly growing with the (Euclidean) distance to the critical point and is 0 at the critical point. Therefore, the density map from a center critical point onto the PCD does not reveal a discontinuity. Besides, an alternative explanation for this is given by the smoothness effect: since a center discontinuity yields an edge curve within the DD [18], it cannot be a discontinuity within the PCD.

A saddle critical point corresponds to the introduced 3D's minimum behavior of the contour integral $f(s, \eta_1)$: The density φ has a local maximum at the critical point which decreases with the (Euclidean) distance to the critical point. Therefore, the density map from a saddle critical point onto the CPC does not reveal a discontinuity, but a local maximum curve, a so-called ridge curve (cf. [21]). This is an unexpected result because it means that discontinuity features completely disappear within a corresponding CPC.

Finally, one special case needs to be discussed. If a CSP^{3D} based on the SDs of a CSP^{2D} would be created just by stacking the two-dimensional SDs one above the other, then the critical points in ∇s would become features lines. However, such feature lines would be structurally unstable and disappear by adding noise.

5.3.3 Numerical Considerations about the CPC Rendering

During the CPC rendering, the numerical quantification error might cause a poor sampling of lathy smooth regions within the PCD's density. The more lathy the regions are, the stronger this effect might be. In our discussion, this effect mainly concerns the edge curves in DD, which correspond to a “quickly fallen” density function in PCD. A poor quantification depends on the sampling's resolution and yields pseudo edges within the CPC which we denote as *shadow edges*. From our experience, shadow edges are mainly weak artifacts which are getting weaker by increasing resolution.

5.3.4 CPC Feature Curves Detection Algorithm

The CSP attract curves form also feature curves in the CPC and thus need to be detected. In [18], algorithmic approaches have been introduced in order to detect the CSP's feature curves. By applying these approaches, a feature curve is approximately given by a polyline \mathbf{L} . Through the curve-curve duality we know that curves of the involved domains are related. Therefore, we have to map the polyline \mathbf{L} in DD onto the corresponding polyline in PCD, which approximates the corresponding curve in CPC.

A single line segment $\mathbf{L}_i; i = 1, \dots, k$, with a startpoint/endpoint $\mathbf{L}_{i_s} = (\xi_{1,i_s}, \xi_{2,i_s})^T$ and $\mathbf{L}_{i_e} = (\xi_{1,i_e}, \xi_{2,i_e})^T$ can be interpreted as the first order approximation of the tangent vector on the DD's feature curve at a certain point. With the aid of Equation (4) the corresponding curve point \mathbf{L}_i in PCD can be approximately calculated by:

$$\mathbf{L}_i = \begin{pmatrix} 0 \\ \xi_{1,i_s} \end{pmatrix} + \frac{\xi_{1,i_e} - \xi_{1,i_s}}{(\xi_{1,i_e} - \xi_{1,i_s}) - (\xi_{2,i_e} - \xi_{2,i_s})} \cdot \begin{pmatrix} 1 \\ \xi_{2,i_s} - \xi_{1,i_s} \end{pmatrix}.$$

The polyline \mathbf{L} approximates the corresponding discontinuity curve in PCD with its line segments given by $\mathbf{L}_i/\mathbf{L}_{i+1}$.

5.3.5 Summary of the Feature Considerations

In this section we briefly summarize the investigations of features in CPCs. First, the local features do not generate stable features. Furthermore, global features as attract curves of a $CSP^{2D/3D}$ form features stable within the CPC. Nevertheless, the attract curves of CSP^{3D} do not map on discontinuity curves in CPC. Furthermore, edge curves in general disappear due to the smoothness effect, but – depending on the resolution – they might produce weak shadow edges. Figure 17 summarizes the classification and their relations concerning the features.

CSP^{2D}	CPC
attract curve $\sigma(\xi) = \infty$ (discontinuity)	appear as
case 1: center line in $s(x, y, \eta_1)$	→ edge curve (discontinuity)
case 2: saddle line in $s(x, y, \eta_1)$	→ attract curve $\varphi(\eta) = \infty$ (discontinuity)
CSP^{3D}	CPC
attract curve $\sigma(\xi) = \infty$ (saddle discontinuity in \mathbf{q})	→ ridge curve (no discontinuity)
edge curve (center discontinuity in \mathbf{q})	→ disappear due to smoothness effect but in practice: might appear as shadow edge
$CSP^{2D/3D}$	CPC
edge curve (caused by boundary effects)	→ disappear due to smoothness effect but in practice: might appear as shadow edge

Fig. 17. Classification of the mapping of global features from $CSP^{2D/3D}$ onto CPC. It is salient that only attract curves (infinite density) of CSP form feature curves in the CPC.

6 APPLICATIONS

We illustrate the introduced features and concepts regarding their relations, in this section. The CPCs/CSPs are calculated on an Intel Core 2 Quad CPU in single core mode, with Linux OS and 3.5 GB RAM, by using the approaches of [3, 4]/[14]; interpolations are done by radial basis function [8], and the features are calculated by [18] and the approach of Section 5.3.4.

Figure 13 shows an example of the linked overlay tool (c.f. Section 4.2) for the CSP_1^{2D} , with the underlying DD scalar fields:

$$CSP_1^{2D} := \begin{pmatrix} \xi_1(\mathbf{x}) = \sin(x) \cdot x + \cos(y) \cdot y \\ \xi_2(\mathbf{x}) = \cos(x) \cdot y + \sin(y) \cdot x \end{pmatrix}. \quad (10)$$

From our theses in Section 5 it follows that a point on a feature curve in one domain has to correspond to the tangent line of the corresponding feature point in the other domain. This property can be simply shown with the aid of our overlay tool by converging a radius against zero for a point of interest. Using the point-line duality directly is not advisable due to numerical reasons. However, it can be seen that this property applies. Furthermore, other scientists can check our theses too with minimal effort, just by using this linked overlay tool.

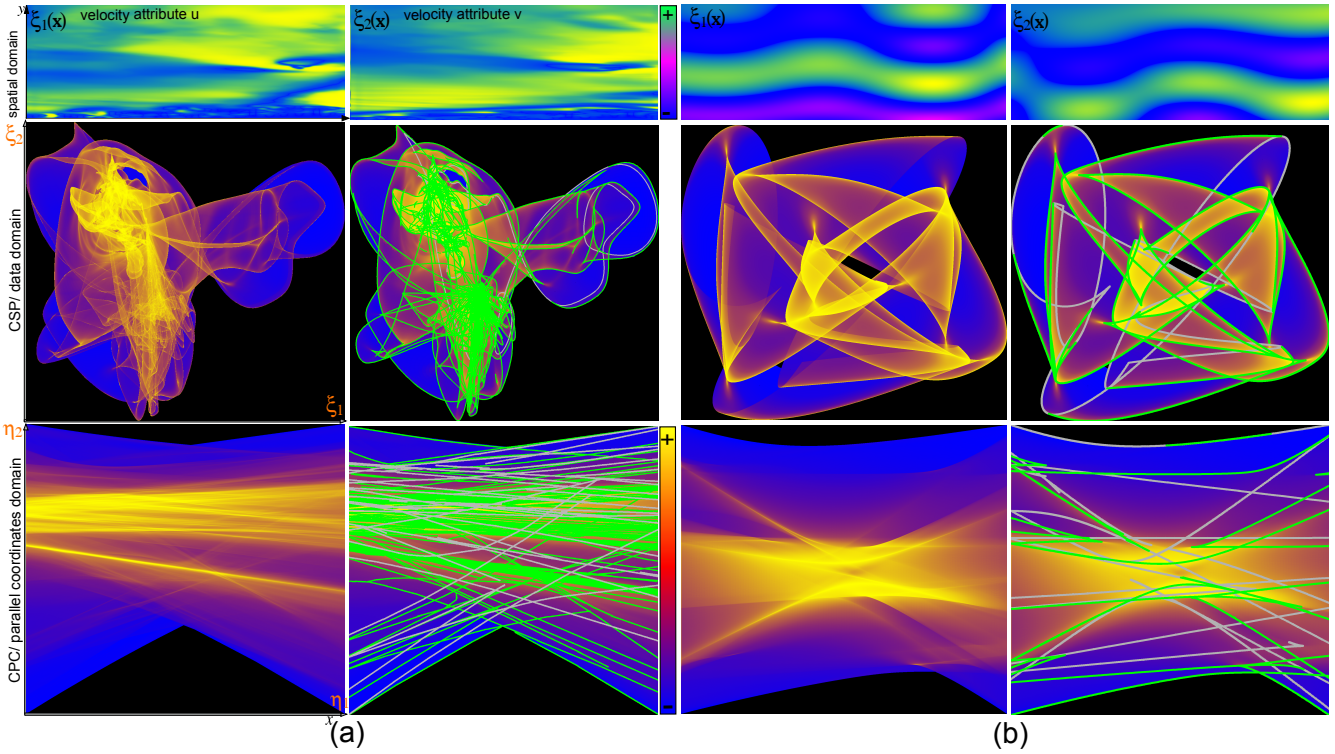


Fig. 15. 2D Applications: (a) Example of “North Sea” data and (b) of synthetic scalar fields. (a/b,up) Visualization of “North Sea”/scalar field data. (a/b,middle-left) $CSP_{\text{north}}^{2D}/CSP_2^{2D}$ and (a/b,middle-right) with green/gray colored attract/edge curves. (a/b,down-left) The corresponding CPC and (a/b,down-right) with green/gray colored counterparts of the attract/edge curves, generated by the curve-curve duality: Attract curves of the CSP correlate with feature curves of the CPC and are dominant, while edge curves disappear (smoothness effect), except weak shadow edges.

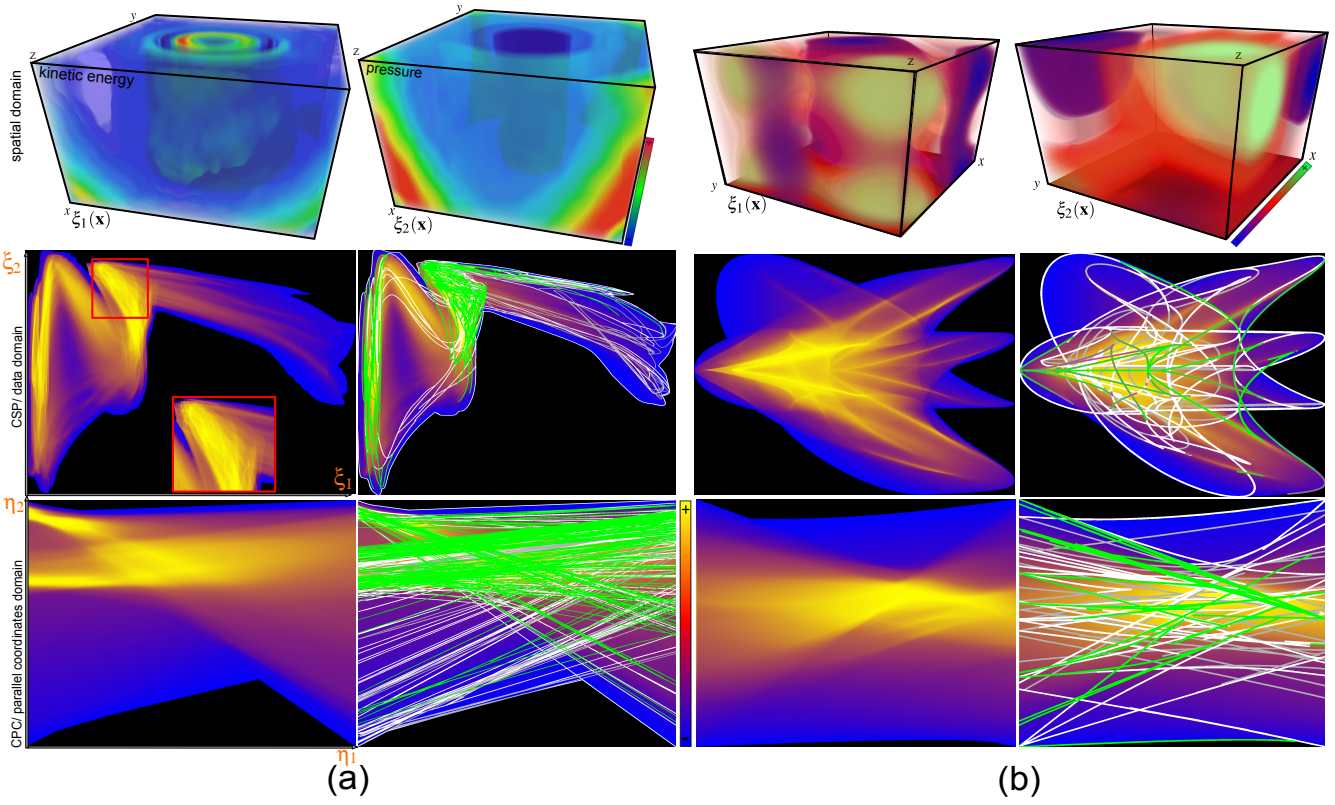


Fig. 16. 3D Applications: (a) Example of “Cyclone” data and (b) of synthetic scalar fields. (a/b,up) Visualization of “Cyclone”/scalar field data. (a/b,middle-left) $CSP_{cycl}^{3D}/CSP_2^{3D}$ and (a/b,middle-right) with green/gray-white colored attract/edge curves. (a/b,down-left) The corresponding CPC and (a/b,down-right) with green/gray-white colored counterparts of the attract/edge curves: There are no correlations between CSP/CPC feature curves, except saddle discontinuity-based attract curves; they do manifest as CPC’s maximum curves (ridges) or shadow edges, respectively.

Figure 15 shows different results for the 2D case: the first example yields the $\text{CSP}_{\text{north}}^{2D}$, based on the topmost slice of the “North Sea” data set, which include flow information of the German Bight from 10/17/2008 (cf. [18, 19]). The second example yields the CSP_2^{2D} based on a SD range of $[1, 10] \times [1, 10]$ and a resolution of 1600×1600 , where the underlying scalar fields of the DD are given by:

$$\text{CSP}_2^{2D} := \begin{pmatrix} \xi_1(\mathbf{x}) = \sin(y) \cdot \sin(x) \cdot x + \cos(y) \cdot y \\ \xi_2(\mathbf{x}) = \cos(y) \cdot \cos(x) \cdot y + \sin(x) \cdot x \end{pmatrix}.$$

It can be seen that the CSP’s attract curves either link to CPC’s attract curves (saddle case) or edges curves (center case). In general, there is a strong correlation between the attract curves of CSP and the features of CPC. That applies also for the number of features in the different domains (compare Figure 15 (a) with (b)): A larger feature number in one domain also reveals a larger number of features within the other domain. Furthermore, the CSP edge curves disappear within the CPC due to the smoothness effect, except for some weak shadow edges.

Figure 16 shows several results for the 3D case: the first example yields the $\text{CSP}_{\text{cycl}}^{3D}$, based on the “Cyclone” data set [22], which includes among others information about pressure and kinetic energy of a physical flow simulation of a hydrocyclone (over a 127^3 SD). The second example yields the CSP^{3D} based on a SD range of $[-2, 3] \times [-2, 3] \times [-2, 3]$ and a resolution of 1400×1400 , where the underlying scalar fields of the DD are given by:

$$\text{CSP}_2^{3D} := \begin{pmatrix} \xi_1(\mathbf{x}) = \sin(z) \cdot \sin(x) \cdot x + \sin(y) \cdot y + \sin(z) \cdot z \\ \xi_2(\mathbf{x}) = \sin(z) \cdot \sin(x) \cdot y + \sin(y) \cdot x + \sin(z) \cdot y \end{pmatrix}.$$

In comparison to the CPC of the 2D case, the CPC of the 3D case looks generally more blurred (cf. Section 5.3). It can be seen that only the CSP’s attract curves (saddle discontinuities) link to smooth maximum density curves within the CPC, or form shadow edges in certain circumstances. All further features, as boundary curves or center discontinuities, disappear. Also the number of CSP features does not correlate to the number of the few CPC features (compare Figure 16 (a) with (b)). Altogether, it confirms that only the attract curves of $\text{CSP}^{2D/3D}$ have a counterpart within the CPCs.

7 DATA ANALYSIS BY CSP/CPC: A FEW CONSIDERATIONS

In this section we discuss the progress concerning the data analysis with CSPs/CPCs.

Article [18] has shown that the number of inverse image elements of map function τ changes at discontinuity curves of a $\text{CSP}^{2D/3D}$. Since the features of CSP map onto features in the CPC, the same statement also applies for them (*inverse image property*). Since the CSPs/CPCs are appropriate as visualization method for a variety of data sets, e.g., physical, statistical, or other, it is not trivial to figure out what this abstract semantic property means for a certain case. Nevertheless, these structures are in the data, thus relevant for the analysis, and detectable by those features.

Furthermore, the SD boundary edges always yield edge curves in the $\text{CSP}^{2D/3D}$ as visual result of the SD’s finiteness. Thus, the CSP edge curves are not relevant for the data analysis because they have nothing to do with the data. On the contrary, the attract curves are really caused by the data. The mapping function τ between SD and DD is always based on the underlying data and consequently the (data-based) attract curves represent characteristics of the data. Figure 18 illustrates the CSP_1^{2D} (Equation (10)) and CSP_1^{3D} , which consists of the following two DD scalar fields

$$\text{CSP}_1^{3D} := \begin{pmatrix} \xi_1(\mathbf{x}) = \sin(x) \cdot x + \sin(y) \cdot y + \sin(z) \cdot z \\ \xi_2(\mathbf{x}) = \sin(x) \cdot y + \sin(y) \cdot x + \sin(z) \cdot y \end{pmatrix}.$$

It can be seen that the attract curves are characteristic for the underlying scalar fields, while the boundary caused edge curves are volatile and unspecific.

There is one special case concerning the CSP^{3D} which needs to be further discussed: the center discontinuities (cf. Figure 1). One

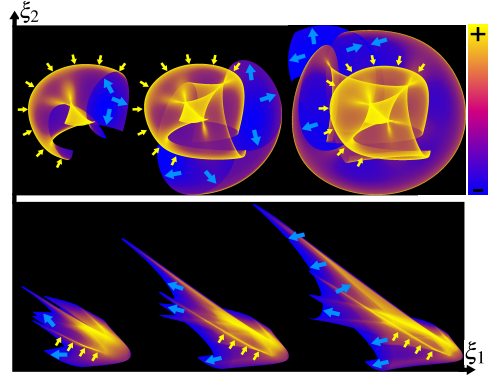


Fig. 18. Relevance of CSP’s discontinuity features: (up, left to right) CSP_1^{2D} of spatial domain $\mathbf{x} \in \{1, 6\}$, $\mathbf{x} \in \{1, 8\}$, and $\mathbf{x} \in \{1, 10\}$. (down, left to right) CSP_1^{3D} of spatial domain $\mathbf{x} \in \{1, 3\}$, $\mathbf{x} \in \{1, 3.5\}$, and $\mathbf{x} \in \{1, 4\}$: The data characteristic attract curves (yellow arrows) remain at the same position and resize depending on the considered SD while edge curves (blue arrows) are volatile and unspecific.

the one hand, they form edge curves, and on the other hand they are caused by the data-based mapping function τ . Are they also relevant for the analysis? Not necessarily, as we will explain as follows: A center discontinuity is a by-product of two saddle discontinuities [18] due to the mathematical properties of the underlying vector field \mathbf{q} . Shannon [23] points out that information is the measure of unpredictability. If there are two saddle discontinuities, it is predictable that there is one center discontinuity belonging to them, i.e., no further information about the data is available. Furthermore, the pathway of the saddle discontinuities specifies the pathway of the corresponding center discontinuity, i.e., also no further information about the data is available. In summary, neither the existents nor the pathway of the center discontinuities contain more or new information as the corresponding saddle discontinuities already convey. Finally, it follows for $\text{CSP}^{2D/3D}$ that the attract curves are relevant for the data analysis. Fortunately, those attract curve features, which are relevant for the data analysis, remain in a CPC (cf. Figure 17), while non-relevant edge curve features disappear due to the smoothness effect: a CPC conveys only relevant features (*relevance property*), a CSP conveys relevant as well as non-relevant features. This shows an advantage of the CPCs in comparison to the CSPs and concerning the data analysis.

8 CONCLUSION AND FUTURE WORK

In this paper, we investigated the features of CPCs, their classification, and their relations to known CSP features. With the linked overlay tool we proposed a method to check our theses by other scientists, and gave an algorithmic detection approach for the CPC features based on the curve-curve duality. Additionally, we described the smoothness effect which blurred CSP edges, and shadow edges caused by numerical reasons. Concluding, we introduced the inverse image property and the relevance property of CPCs, which are new contributions concerning the task of a CPC/CSP-based data analysis.

The statement of the paper is that only CSP’s attract curves – which are the relevant features concerning the data analysis – map stable and form the dominant CPC features, while other features disappear. Thus, especially for unexperienced users the CPC is less confusing.

What remains for the future is to develop feature-based reconstruction approaches for CPC/CSP and appropriate Linking & Brushing [6] tools for CPCs, in order to investigate further properties between features and underlying data to further improve the task of data analysis. Additionally, the analysis of the features for CPCs/CSPs concerning time-dependent multivariate data will be done.

ACKNOWLEDGMENTS

This work was supported by a grant from the German Science Foundation (DFG), project DFG TH692/6-1.

REFERENCES

- [1] B. Ackland and N. Weste. Real time animation playback on a frame store display system. In *Proceedings of the 7th annual conference on Computer graphics and interactive techniques*, SIGGRAPH '80, pages 182–188, New York, NY, USA, 1980. ACM.
- [2] S. Bachthaler, S. Frey, and D. Weiskopf. Poster: Cuda-accelerated continuous 2d scatterplots. *IEEE Visualization Conference*, 2009.
- [3] S. Bachthaler and D. Weiskopf. Continuous scatterplots. *IEEE Transactions on Visualization and Computer Graphics (Proceedings Visualization / Information Visualization 2008)*, 14(6):1428–1435, November – December 2008.
- [4] S. Bachthaler and D. Weiskopf. Efficient and adaptive rendering of 2-d continuous scatterplots. *Computer Graphics Forum*, 28(3):743–750, 2009.
- [5] C. L. Bajaj, V. Pascucci, and D. R. Schikore. Visualization of scalar topology for structural enhancement. In *Proc. of IEEE Visualization*, pages 51–58, 1998.
- [6] R. Becker and W. Cleveland. Brushing scatterplots. *Technometrics*, 29,2:127–142, 1987.
- [7] P.-T. Bremer, H. Edelsbrunner, B. Hamann, and V. Pascucci. A topological hierarchy for functions on triangulated surfaces. *IEEE Transactions on Visualization and Computer Graphics*, 10(4):385–396, 2004.
- [8] J. C. Carr, R. K. Beatson, J. B. Cherrie, T. J. Mitchell, W. R. Fright, B. C. McCallum, and T. R. Evans. Reconstruction and representation of 3d objects with radial basis functions. *SIGGRAPH 2001: Proceedings of the 28th annual conference on Computer graphics and interactive techniques*, pages 67–76, 2001.
- [9] H. Edelsbrunner, J. Harer, and A. Zomorodian. Hierarchical morse-smale complexes for piecewise linear 2-manifolds. *Discrete and Computational Geometry*, 30(1):87–107, 2003.
- [10] J. D. Foley, A. van Dam, S. K. Feiner, and J. F. Hughes. *Computer Graphics: Principles and Practice*. Addison-Wesley, Reading, MA, 2 edition, 1990.
- [11] R. Forman. Morse theory for cell-complexes. *Advances in Mathematics*, 134,1:90–145, 1998.
- [12] R. Forman. A user's guide to discrete morse theory. *Sminaire Lotharingien de Combinatoire*, B48c, 2002.
- [13] J. Heinrich, S. Bachthaler, and D. Weiskopf. Progressive splatting of continuous scatterplots and parallel coordinates. *Computer Graphics Forum (Proceedings EuroVis 2011)*, 30(3), 2011.
- [14] J. Heinrich and D. Weiskopf. Continuous Parallel Coordinates. *IEEE Transactions on Visualization and Computer Graphics (Proceedings Visualization / Information Visualization 2009)*, 15(6):1531–1538, 2009.
- [15] A. Inselberg. The plane with parallel coordinates. *The Visual Computer*, 1(2):69–91, 1985.
- [16] A. Inselberg. Parallel coordinates. *Publisher Springer Berlin*, 2009.
- [17] A. Inselberg and B. Dimsdale. Multidimensional lines 2: Proximity and applications. *SIAM Journal on Applied Mathematics*, 54(2):578–596, 1994.
- [18] D. J. Lehmann and H. Theisel. Discontinuities in continuous scatterplots. *IEEE Transactions on Visualization and Computer Graphics (Proceedings IEEE Visualization)*, 16(6):1291–1300, 2010.
- [19] M. Otto, T. Germer, H.-C. Hege, and H. Theisel. Uncertain 2d vector field topology. In *Computer Graphics Forum (Proceedings of Eurographics 2010)*, volume 29, pages 347–356, Norrkping, Sweden, 5 2010.
- [20] R. Peikert and M. Roth. The Parallel Vectors Operator - A Vector Field Visualization Primitive. In *Proceedings of the 10th IEEE Visualization Conference (VIS '99)*, volume 0, pages 263–270, Washington, DC, USA, 1999. IEEE Computer Society.
- [21] R. Peikert and F. Sadlo. Height Ridge Computation and Filtering for Visualization. In *Proceedings of Pacific Vis 2008*, pages 119–126, March 2008.
- [22] M. Ruetten. Cyclone data set: physical flow simulation within a hydrocyclone, realized at institute of aerodynamics, german aerospace center.
- [23] C. Shannon. A mathematical theory of communication. *Bell Systems Techn. Journal*, 27:623–656, 1948.
- [24] H. Theisel. *CAGD and Scientific Visualization*. Habilitation theses, University of Rostock, Computer Science Department, 2001.
- [25] H. Theisel and H.-P. Seidel. Feature flow fields. In G.-P. Bonneau, S. Hahmann, and C. H. (Ed.), editors, *Proc. Joint Eurographics - IEEE TCVG Symposium on Visualization (VisSym'03)*, pages 141–148, 2003.
- [26] T. Weinkauf. *Extraction of Topological Structures in 2D and 3D Vector Fields*. PhD thesis, University Magdeburg, 2008.
- [27] T. Weinkauf, H. Theisel, A. V. Gelder, and A. Pang. Stable feature flow fields. *IEEE Transactions on Visualization and Computer Graphics*, 17:770–780, 2011.
- [28] T. Weinkauf, H. Theisel, H.-C. Hege, and H.-P. Seidel. Boundary switch connectors for topological visualization of complex 3d vector fields. In: *Proc. Joint Eurographics - IEEE TCVG Symposium on Visualization (VisSym'04)*, pages 183–192, 2004.